The Role of the N Terminus and Transmembrane Domain of TRPM8 in Channel Localization and Tetramerization

THE JOURNAL OF BIOLOGICAL CHEMISTRY VOL. 282, NO. 50, pp. 36474–36480, December 14, 2007

The Role of the N Terminus and Transmembrane Domain of TRPM8 in Channel Localization and Tetramerization*[S]

Received for publication, August 28, 2007, and in revised form, September 26, 2007 Published, JBC Papers in Press, October 1, 2007, DOI 10.1074/jbc.M707205200

Christopher B. Phelps and Rachelle Gaudet[1]

From the Department of Molecular and Cellular Biology, Harvard University, Cambridge, Massachusetts 02138

Transient receptor potential (TRP) channels are a family of cation channels involved in diverse cellular functions. They are composed of a transmembrane domain of six putative transmembrane segments flanked by large N- and C-terminal cytoplasmic domains. The melastatin subfamily (TRPM) channels have N-terminal domains of ~700 amino acids with four regions of shared homology and C-terminal domains containing the conserved TRP domain followed by a coiled-coil region. Here we investigated the effects of N- and C-terminal deletions on the cold and menthol receptor, TRPM8, expressed heterologously in Sf21 insect cells. Patch-clamp electrophysiology was used to study channel activity and revealed that only deletion of the first 39 amino acids was tolerated by the channel. Further N-terminal truncation or any C-terminal deletions prevented proper TRPM8 function. Confocal microscopy with immunofluorescence revealed that amino acids 40–86 are required for localization to the plasma membrane. Furthermore, analysis of deletion mutant oligomerization shows that the transmembrane domain is sufficient for TPRM8 assembly into tetramers. TRPM8 channels with C-terminal deletions tetramerize and localize properly but are inactive, indicating that although not essential for tetramerization and localization, the C terminus is critical for proper function of the channel sensor and/or gate.

The cold and menthol receptor, TRPM8 (also called CMR1 or Trp-p8), is a member of the transient receptor potential (TRP)[2] family of cation channels. TRP channels are involved in a broad range of cellular processes. The mammalian TRP family consists of 28 known members divided into six subfamilies (TRPA, -C, -M, -ML, -P, and -V) (1). Many TRP channels act as cellular sensors that respond to stimuli ranging from physical and mechanical (*e.g.* temperature or the osmotic pressure of a cell) to chemical stimuli (2, 3).

All TRP channels contain six predicted transmembrane segments, S1 to S6, flanked by cytoplasmic N- and C-terminal domains. Shared homology in these N- and C-terminal regions is what defines the different TRP subfamilies. The transmembrane region is predicted to form tetrameric channels and share a similar fold to voltage-dependent K^+ channels (4, 5). Most TRP channels also have a short hydrophobic "TRP domain" sequence shortly after the last transmembrane segment (1, 6). Unlike the TRPC and TRPV channels, which contain between three and six ankyrin repeats in their N-terminal cytoplasmic domains, TRPM8 and the seven other TRPM channels share four regions of high homology (TRPM homology regions, MHRs) in their N-terminal cytoplasmic domain (3, 7). The TRPMs also have a coiled-coil region just C-terminal to the TRP domain (7). TRPM proteins are involved in a broad range of biological processes, such as responses to oxidative stress (TRPM2), T-cell activation (TRPM4), taste (TRPM5), magnesium homeostasis (TRPM6 and TRPM7), and temperature sensation (TRPM8) (8, 9).

TRPM8 is activated by "cool" temperatures (8–25 °C) and "cooling" agents such as menthol, eucalyptol, and icilin (10, 11), and TRPM8 knock-out mice are impaired in cold sensation (12–14). The depolarization of sensory neurons expressing TRPM8 is a result of Na^+ influx through the channel because of the much higher extracellular concentration of Na^+ *versus* Ca^{2+} and the low selectivity of TRPM8 ($P_{Ca/Na} = 3.2$) (10, 15). The TRPM8 temperature response is mediated at least in part by its C-terminal intracellular domain: chimeras swapping the C-terminal domains of TRPM8 and TPRV1 (*i.e.* the vanilloid family TRP channel activated by temperatures >42 °C (16)) switch their thermal sensitivity (17). These chimeras retained their wild-type chemical agonist sensitivity.

TRPM8 gating is not regulated by temperature alone. Voltage and pH interact allosterically with temperature to activate the channel (18–20). TRPM8 and other TRP channels are voltage-dependent and can be activated upon depolarization. In fact, cooling and ligand binding lead to TRPM8 channel opening by shifting of the activation voltage into the physiologic range (18). Mutagenesis indicates that the voltage sensor is in the S4 and S4–S5 linker, and mutation of residues involved in voltage sensation also alters the temperature and agonist sensitivity (21). The two best characterized chemical agonists of TRPM8, icilin and menthol, activate the channel through distinct mechanisms. Activation by icilin is inhibited by low pH and by the absence of intracellular Ca^{2+}. On the other hand, menthol activation is unaffected by pH and is inhibited by the presence of intracellular Ca^{2+} (22, 23). Mutational analyses indicate that residues in the S1 and S2 transmembrane segments are required for TRPM8 activation by menthol and icilin (22, 24) and that residues in the S4 transmembrane segment and S4–S5

* This work was supported by McKnight Scholar and Klingenstein Fellowship awards (to R. G.). The costs of publication of this article were defrayed in part by the payment of page charges. This article must therefore be hereby marked "*advertisement*" in accordance with 18 U.S.C. Section 1734 solely to indicate this fact.

[S] The on-line version of this article (available at http://www.jbc.org) contains supplemental Fig. S1.

[1] To whom correspondence should be addressed: Dept. of Molecular and Cellular Biology, Harvard University, 7 Divinity Ave., Cambridge, MA 02138. Tel.: 617-495-5616; Fax: 617-496-9684; E-mail: gaudet@mcb.harvard.edu.

[2] The abbreviations used are: TRP, transient receptor potential; MES, 2-(*N*-morpholino)ethanesulfonic acid; MHR, melastatin subfamily channel homology region; PFO, pentadecafluorooctanoic acid; PIP_2, phosphatidylinositol 4,5-bisphosphate; pF, picofarad.

linker are also important for menthol binding (21). In addition, hydrophobic residues in the TRP domain are important for menthol, but not temperature, activation (24). Finally, phosphatidylinositol 4,5-bisphosphate (PIP_2) is required for TRPM8 activity. Hydrolysis of PIP_2 after TRPM8 activation and the resulting Ca^{2+} entry into the cells results in rundown of the TRPM8 current (25). Current evidence indicates that conserved positively charged residues in the TRP domain are involved in the PIP_2 regulation of TRPM8 and other TRP channels (26).

In this study we endeavored to determine the role of different TRPM8 regions. This was carried out by deletion mutagenesis in combination with assays for channel function: tetramerization, localization, and channel activation by cooling and agonists. Both the N and C termini of TRPM8 are critical for proper function. A region N-terminal to the first MHR, encompassing residues 40–86, is required for plasma membrane localization. Furthermore, although the transmembrane domain is sufficient for tetramerization, the C-terminal coiled-coil domain is an important component of the channel gate.

MATERIALS AND METHODS

Cloning and Expression—Using the QuikChange PCR protocol (Stratagene), the silent mutations c198t and t2772c were introduced into *Rattus norvegicus* TRPM8 cDNA (provided by David Julius) to remove two NdeI sites. Full-length TRPM8 and the deletion mutants were amplified by PCR and ligated between the NdeI and NotI sites of a modified pFastBac1 vector, pFastBac-CFLAG, with an altered multiple cloning site and encoding a C-terminal FLAG tag (27). Bacmid DNA was produced by transformation of the resulting pFBF1-TRPM8 DNA vectors into DH10Bac cells and then transfected into Sf21 insect cells using standard protocols to produce baculovirus (Invitrogen). Insect cells were grown at 27 °C in Hink's TNM-FH (Mediatech) supplemented with 10% fetal bovine serum and 0.1% Pluronic F-68.

Electrophysiology—Insect cells were adhered to 12-mm glass coverslips and infected with baculovirus carrying full-length TRPM8 or the deletion mutants at a multiplicity of infection providing maximal protein expression. Currents were recorded 48–52 h postinfection using 2–4 megaohms resistance borosilicate pipettes in the whole-cell patch-clamp configuration on an Axopatch 200B amplifier controlled by a Digidata 1322 and pClamp 9.2 software (Molecular Devices) with data sampling at 5–10 kHz. Whole-cell capacitance was recorded from the amplifier settings. Voltage ramps (1500 ms) from −100 to +100 mV were applied every 5 s from a holding potential of 0 mV. Data were analyzed and displayed with Origin 7.0 (OriginLab Corp.) or pClamp 9.2 software. Cells were placed in a temperature-controlled chamber with the thermistor within 1 mm of the recorded cell and held at 28 °C or subjected to temperature ramps by continuous perfusion. A CL-100 bipolar temperature controller (Warner Instruments) was used to control the electrophysiology chamber temperature and generate temperature ramps. A multichamber perfusion apparatus was used for agonist application. The bath (perfusion) solution contained 140 mM sodium gluconate, 10 mM MES, 2 mM $CaCl_2$, 1 mM $MgCl_2$, and 10 mM D-glucose, adjusted to pH 6.3 with NaOH and an osmolarity of 315 mosM with NaCl. The pipette solution contained 140 mM cesium methanesulfonate, 10 mM MES, 2.5 mM NaCl, and 10 mM EGTA, adjusted to pH 6.3 with CsOH and an osmolarity of 315 mosM. For pH 7.2 experiments, the MES was replaced with HEPES in both the pipette and bath solutions. Menthol (Sigma) and icilin (Tocris) were dissolved in Me_2SO prior to dilution in the bath solution. The concentration of Me_2SO in the bath solution was <0.1%, and controls showed no response to Me_2SO alone. Data are presented as mean ± S.E.

Immunofluorescence with Confocal Laser Scanning Microscopy—Insect cells were allowed to grow overnight on 22-mm coverslips before baculovirus infection with FLAG-tagged TRPM8. The virus was aspirated and replaced with fresh medium after 1 h to ensure synchronous infection and expression. After 48 h the cells were fixed with formaldehyde, permeabilized with saponin, stained with monoclonal anti-FLAG antibody M2-fluorescein isothiocynate conjugate (Sigma), and counterstained with Hoechst 33342 (Molecular Probes). Slides were mounted using ProLong solution (Molecular Probes). Images were collected within 48 h of staining/mounting using a Zeiss LSM510 META on an upright microscope with 355- and 488-nm lasers at the Harvard University Department of Molecular and Cellular Biology Imaging Facility.

Pentadecafluorooctanoic Acid (PFO)-PAGE—Insect cells were infected as for immunofluorescence, washed once with Tris-buffered saline, homogenized in Tris-buffered saline + 1% Triton X-100, and centrifuged to remove cell debris. Whole-cell lysates were mixed with an equal volume of PFO sample buffer (100 mM Tris, 20% glycerol, 8% PFO (Fluka), and 0.005% bromphenol blue (pH 8.0)) and run on a 4–15% gel in 20 mM Tris, 192 mM glycine, and 0.5% PFO (pH 8.3). FLAG-tagged TRPM8 constructs were detected by Western blotting using anti-FLAG antibody M2 conjugated to alkaline phosphatase (Sigma).

Anti-FLAG M2-Agarose Pulldowns and Size Exclusion Chromatography—Insect cells were co-infected with baculovirus carrying the appropriate FLAG-tagged constructs and harvested 48 h postinfection. Cells were lysed by trituration in 50 mM Tris-HCl, 50 mM NaCl, 1 mM EDTA, 1 mM phenylmethylsulfonyl fluoride, and 1% Fos-choline-12 (pH 7.5) (Anatrace) and incubated for 1 h at 4 °C prior to centrifugation for 20 min at 20,000 × *g*. Supernatants were applied to 50 μl of anti-FLAG M2-agarose beads (Sigma) and incubated for 1 h at 4 °C. The beads were washed four times with 1 ml of Tris-buffered saline (pH 7.5) + 1 mM EDTA (pH 8.0), 1 mM phenylmethylsulfonyl fluoride, and 0.2% Fos-choline-12 and eluted with 0.5 ml of the same solution supplemented with 0.2 mg/ml 3X FLAG peptide (Biopolymers Laboratory at Harvard Medical School). The samples were injected on a Sephacryl S300 size exclusion column (GE Healthcare) in Tris-buffered saline (pH 7.4) supplemented with 1 mM EDTA (pH 8.0), 1 mM dithiothreitol, and 0.1% Fos-choline-12. Bio-Rad size exclusion standards were used to calibrate the column. The elution volumes of the TRPM8 samples were determined by Western blotting using anti-FLAG M2-antibody conjugated to alkaline phosphatase (Sigma).

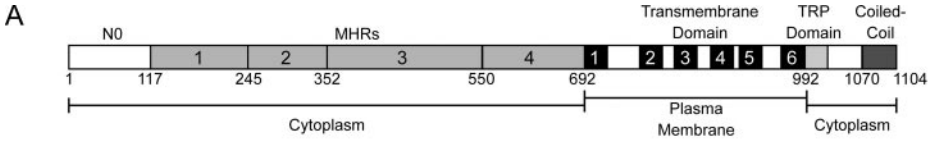

B

Name	Residues	MW (kD)	Tetramer	Plasma Membrane	Menthol (1 mM)	Temperature (12 °C)
M8-FL	1-1104	129	+	+	+	+
ΔN39	40-1104	125	+	+	+	+
ΔN86	87-1104	120	+	-	-	-
ΔN116	117-1104	116	+	-	-	-
ΔN245	246-1104	101	+	-	-	-
ΔN352	353-1104	89	+	-	-	-
ΔC1070	1-1069	125	+	+	-	-
ΔC992	1-991	115	+	+	-	-
M8-NT	1-692	80	-	-	ND	ND

FIGURE 1. **Domain organization of TRPM8 and deletion constructs.** *A*, primary structure of TRPM8, with the MHRs shaded *medium gray*, six transmembrane helices *black*, the TRP domain *light gray*, and the coiled-coil region *dark gray*. *B*, schematic representation and summary of the behavior of TRPM8 deletion mutants assayed in this study. Shading corresponds to *A*.

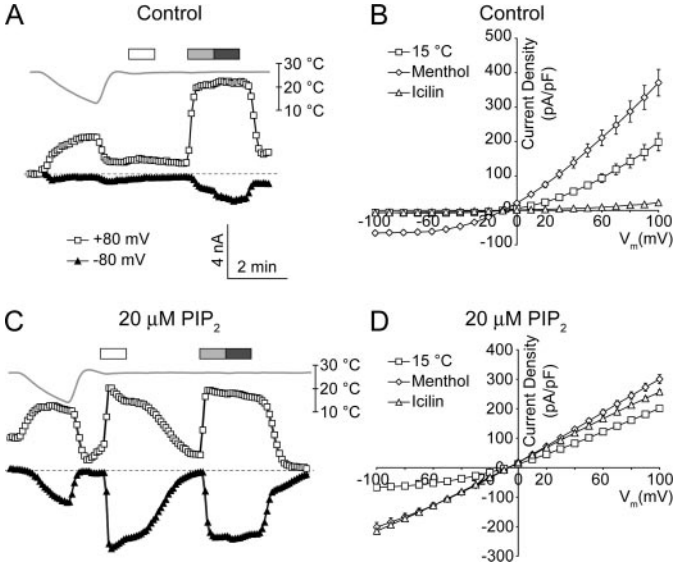

FIGURE 2. **Expression in insect cells does not alter the behavior of TRPM8.** *A*, sample recording from a full-length TRPM8-expressing insect cell at pH 6.3 (control). The currents at +80 (*squares*) and −80 mV (*triangles*) extracted from 1500-ms voltage ramps are shown along with temperature (*gray line*). Indicated above the *trace* is stimulation with 10 μM icilin (*white bar*) or 100 μM (*light gray*) and 500 μM (*dark gray*) menthol in the bath solution. The *dashed line* indicates zero current. *B*, current-voltage relationship for control cells stimulated by temperature (*squares*), 500 μM menthol (*diamonds*), and 10 μM icilin (*triangles*). The current density, extracted from ramps, in pA/pF is plotted against membrane potential V_m (mV) from $n = 6$ cells; *error bars* represent the S.E. *C* and *D*, effects of supplementing the intracellular (pipette) solution with 20 μM PIP_2. The sample recording (*C*) and current-voltage relationship data (*D*) were recorded and processed as in *A* and *B*, and the aggregate data in *D* are from $n = 6$ cells.

RESULTS

Construct Design and Expression—All TRPM8 deletion mutants were generated based on homology to other TRPM family members from worms to humans (alignment in supplemental Fig. S1). The N-terminal deletion mutant boundaries were based on the location of breakpoints in similarity levels. The first deletion, removing the N-terminal 39 residues (ΔN39), marks the start of homology between TRPM8 and other TRPM proteins (Fig. 1). Deletions ΔN86 and ΔN116 remove regions of progressively higher similarity, and residue 117 also marks the start of the first TRPM homology region. The other two N-terminal deletion mutants, ΔN245 and ΔN352, remove the first and second MHRs, respectively. The two C-terminal deletion mutants were designed to remove most of the conserved coiled-coil domain (ΔC1070) and the entire cytosolic region including the TRP domain (ΔC992). The N-terminal cytosolic domain of TRPM8 (M8-NT, residues 1–692) was used as a nontransmembrane domain control. All constructs were cloned with a C-terminal FLAG tag for detection. Full-length FLAG-tagged TRPM8 (M8-FL) and the deletion mutants were expressed in Sf21 insect cells by baculovirus infection, and expression was confirmed by Western blotting (data not shown).

Electrophysiology—TRPM8 activity was assayed using whole-cell patch-clamp electrophysiology in insect cells. Previous studies with TRPV1 have shown the suitability of insect cells for studying TRP channels by electrophysiology (27, 28). Unless otherwise noted, experiments were carried out at the native pH (6.3) of Sf21 insect cells.

TRPM8 expressed in insect cells has a reverse potential of −8.5 ± 2.3 mV and a temperature of 50% activation of 21 ± 2 °C (Fig. 2) similar to the values obtained from mammalian cells (10). At pH 6.3, TRPM8 was activated both by cooling (to 15 °C) and by menthol (0.5 mM). Icilin (10 μM) was unable to activate TRPM8 at pH 6.3 ($n = 6$) (Fig. 2) as observed previously (23). Raising both the intra- and extracellular pH to 7.2 restored sensitivity to icilin but did not alter the response to menthol. At −80 mV, the average maximal current density in response to 0.5 mM menthol is the same, within error, at pH 6.3 and 7.2: −64.5 ± 6.2 pA/pF ($n = 6$) and −70.7 ± 19.2 pA/pF ($n = 4$), respectively. In contrast, there was almost no response to 10 μM icilin at pH 6.3, with a current density of −6.4 ± 1.1 pA/pF ($n = 6$), whereas at pH 7.2 the icilin response was similar to the menthol response, with a current density of −73.3 ± 15.8 pA/pF ($n = 4$). These data confirm that the properties of TRPM8 expressed in insect cells are very similar to those observed previously in mammalian cells (10, 11, 22, 23).

As previous reports indicated that PIP_2 is important for TRPM8 activation, we tested the effect of supplementing the pipette (intracellular) solution with 20 μM PIP_2. In the presence of PIP_2, icilin (10 μM) was able to activate TRPM8 at pH 6.3 with currents almost identical to those activated by menthol in the presence of PIP_2 (Fig. 2). PIP_2 also potentiated the responses to temperature and menthol: much larger currents were observed at negative potentials, and the responses became less outwardly rectified (Fig. 2). These results, combined with other data published previously (19, 21–23, 25), clearly indicate that gating of TRPM8 is modulated by the simultaneous interplay of pH, ligand binding (PIP_2, menthol, and icilin), temperature, and

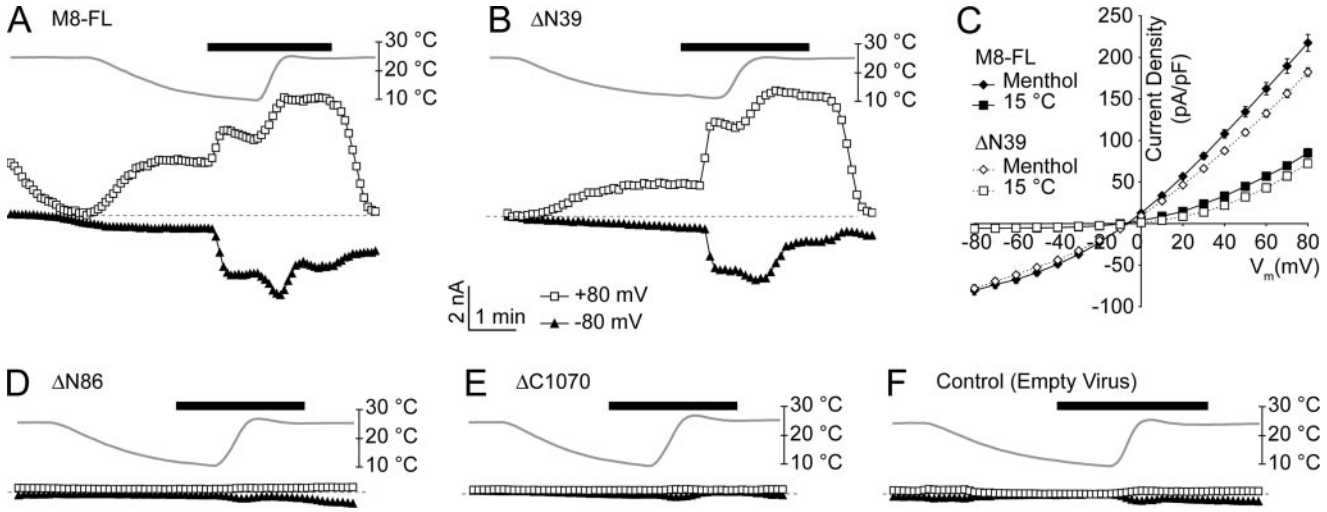

FIGURE 3. **Whole-cell patch-clamp of TPRM8 deletion mutants.** Sample recordings were from insect cells expressing full-length TRPM8 (*A*) or ΔN39 (*B*). *C*, current-voltage relationships of full-length (*solid symbols*) and ΔN39 (*open symbols*) TRPM8 stimulated with 1 mM menthol (*diamonds*) or cooling to 15 °C (*squares*). Average current density is plotted against membrane potential for $n = 8$ cells, *error bars* represent the S.E. *D–F*, sample recordings from insect cells infected with ΔN86 (*D*), ΔC1070 (*E*), and empty virus (control, *F*). ΔN86 and ΔC1070 show the same responses to menthol and temperature as control insect cells infected with empty virus. All currents were extracted from 1500-ms voltage ramps, and currents at +80 (*open squares*) and −80 mV (*filled triangles*) are shown. Temperature is shown in *gray*, and stimulation with 1 mM menthol is indicated by *black bars*. The *dashed lines* indicate zero current.

membrane voltage and that the insect cell expression system is appropriate for the study of TRPM8 and its modulation by all those agonists.

All TPRM8 deletion mutants were then examined for their ability to respond to cooling and menthol (Figs. 1 and 3). Of the deletion mutants, only ΔN39 showed wild-type TRPM8 activity. As shown in Fig. 3, the current-voltage responses for M8-FL and ΔN39 are almost identical for both temperature and menthol. All other mutants failed to respond to either 1 mM menthol or cooling to less than 12 °C. We also applied menthol during cooling, as both stimuli are known to sensitize TRPM8 to the other (10, 11). This sensitization can be seen in the M8-FL and ΔN39 recordings, particularly at a negative potential (Fig. 3). The dual stimulation with temperature and menthol failed to generate a response in all other deletion mutants (Figs. 1*B* and 3). Forty of 46 cells (87%) exposed to M8-FL baculovirus responded to stimulation. Therefore, to eliminate the possibility that the lack of response in other deletion mutants was due to patching of uninfected cells, 10 cells were tested for the smallest truncations (ΔN86, ΔN116, and ΔC1070; a sign test yields a p value of 0.001), and all other deletion mutants were tested six times ($p < 0.05$). In summary, residues 1–39 are dispensable, whereas the conserved regions at the N and C termini of TRPM proteins are critical for the proper functioning of TRPM8.

Tetramerization—To form competent channels that can be studied by patch-clamp electrophysiology, TRPM8 must first form tetramers and be transported to the plasma membrane. Therefore, we endeavored to determine the oligomeric state of the inactive deletion mutants.

Tetramerization was examined using PFO-PAGE. PFO is an anionic detergent that is milder than SDS and preserves the oligomeric structure of many proteins and was shown recently to be effective with TRPM8 (29). Detergent-solubilized insect cell membrane extracts were subjected to PFO-PAGE and visualized by anti-FLAG Western blotting (Fig. 4*A*). Apoferritin, catalase, and bovine serum albumin were also run as molecular weight standards to calculate a standard curve. Fig. 4*B* shows a plot comparing TRPV1 and TRPM8 to molecular weight standards. The relative mobilities of the four observed bands for each TRPV1 and TRPM8 are plotted using the predicted molecular weights of oligomers of $n = 1–4$ and show good agreement with the standards. The N-terminal cytosolic domain was the only construct tested that did not form tetramers.

To confirm the role of the transmembrane domain in subunit association, FLAG-tagged ΔN39 and ΔC1070 were expressed in baculovirus-infected insect cells and partially purified by anti-FLAG pulldown prior to analysis by size exclusion chromatography (Fig. 4*C*). ΔN39 was selected instead of full-length TRPM8 because of its higher expression levels and because it is the active construct that is the closest in molecular weight to ΔC1070. Both ΔN39 and ΔC1070 eluted at approximately the same volume, indicating that they are in the same oligomeric state. Furthermore, their elution volume is consistent with that of a tetramer.

Subcellular Localization—Plasma membrane localization, as mentioned above, is an important step in forming fully functional channels that are accessible to functional assays by patch-clamp electrophysiology. Subcellular localization was determined by confocal microscopy and immunofluorescence (Fig. 5). As expected, the active M8-FL and ΔN39 constructs were localized to the plasma membrane. The other N-terminal deletion mutants were all localized to the intracellular space and were excluded from the nucleus. The staining envelops the nucleus and extends outward in a reticulated pattern consistent with localization to the endoplasmic reticulum and/or Golgi compartments. The N-terminal cytosolic domain of TRPM8 (M8-NT) localized to the cytoplasm and nucleus of insect cells. Combined with the behavior of the constructs in the electrophysiology assays, the subcellular localization of the various N-terminal deletion constructs indicates that the region

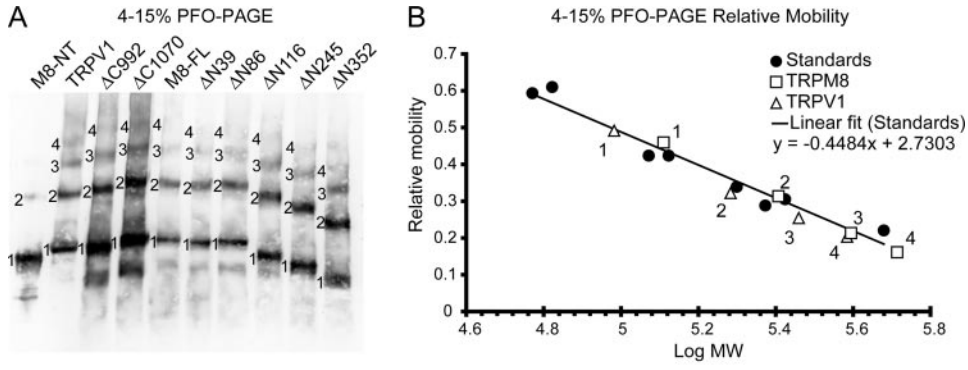

FIGURE 4. **Oligomerization of TRPM8 deletion mutants.** *A*, 4–15% PFO-PAGE visualized by anti-FLAG Western blotting. The number of subunits (*n*) of the oligomers is indicated next to the bands. *B*, relative mobility of PFO-PAGE samples plotted against the log of their molecular weight (*MW*). Standards (apoferritin, catalase, and bovine serum albumin) are shown as *circles*, and the *black line* shows the linear fit to the molecular weight standards. The relative mobilities of TRPV1 (*triangles*) and TRPM8 (*squares*) oligomers are plotted against the calculated molecular weight for *n*-monomers and show good agreement with the standard curve. *C*, 7.5% SDS-PAGE/anti-FLAG Western blotting of fractions from size exclusion analysis of insect cell-expressed ΔN39 and ΔC1070. The void volume (V_0) and retention volumes of molecular weight standards are indicated along with the retention volume of the individual samples.

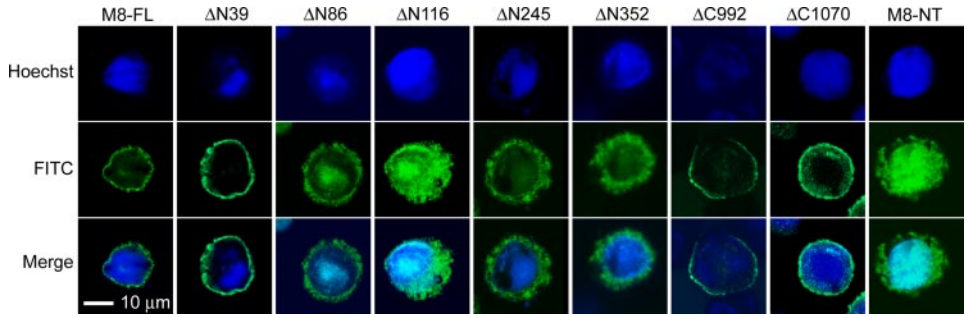

FIGURE 5. **Cellular localization of TRPM8 deletion mutants.** The subcellular localization of immunostained TRPM8 visualized by confocal laser scanning microscopy. Shown are Hoechst (DNA, *blue*), fluorescein isothiocyanate (*FITC*; TRPM8, *green*), and merged images for full-length TRPM8 and the indicated deletion mutants. The *white bar* represents 10 μm.

encompassing residues 40–86 is important for proper TRPM8 localization.

Both C-terminal deletion mutants, ΔC992 and ΔC1070, were localized to the plasma membrane. Therefore, neither the TRP domain nor the coiled-coil domain is required for plasma membrane localization. Given that the C-terminal deletion mutants are capable of tetramerizing and localizing to the plasma membrane but are not activated by ligands or cool temperature, the C-terminal region of TRPM8 is important either for sensing agonist binding and decreased temperature or for gating the channel.

DISCUSSION

Based on our results and recently published data on other TRPM channels, general roles for the N- and C-terminal cytosolic domains can be defined. The region N-terminal to the first MHR is clearly required for proper localization of TRPM8, and similar behavior has been observed for both TRPM2 and TRPM4. Two TRPM2 deletion mutants, similar to ΔN116 and ΔN245, both fail to localize to the plasma membrane (30). Removal of the first 177 residues of TRPM4, which includes MHR1, results in a dominant-negative effect, as expression of TRPM4-ΔN in HEK293 and Jurkat T cells decreased endogenous TRPM4 activity more than 3-fold (31). Our work shows that the N terminus of TRPM8 is also important for plasma membrane localization and has refined the region important for plasma membrane targeting to residues corresponding to 40–86 of TPRM8. These are well conserved in all other TRPM proteins, including those from *Caenorhabditis elegans* (supplemental Fig. S1), except for TRPM1 and TRPM5. Interestingly, a shorter splice variant of TRPM8 that removes the first 65 amino acids, TRPM8b, has been observed in malignant prostate cancer cells (32), and calcium release from the endoplasmic reticulum mediated by TRPM8 has also been observed in these cells (33). It is possible that the alternatively spliced TRPM8b variant is retained in the endoplasmic reticulum, similar to our N-terminal deletion mutants, and remains active in the endoplasmic reticulum. Although residues 40–86 of TRPM8 do not contain a recognizable plasma membrane targeting motif, it is possible that this region is involved in interactions with other proteins that direct TRPM8 to the plasma membrane. Because the N-terminal deletion mutants fail to localize to the plasma membrane, we cannot access them by patch-clamp electrophysiology to determine whether the deletions have any further effects on channel gating and activation. On the other hand, we can be confident that the C-terminal deletions prevent activation and/or opening of TRPM8 channels because they are tetramers that localize to the plasma membrane.

Recent reports on the coiled-coil domain of TRPM8, TRPM2, and TRPM4 have shown that the domain is important for TRPM function (31, 34, 35), and when expressed by itself it is capable of forming tetramers (36). With TRPM2, mutations in the coiled-coil that decrease subunit association also decrease channel activity (34). Removal of the TRPM2 coiled-

coil resulted in a significant, but not complete, reduction in subunit assembly assessed by coimmunoprecipitation of wild type and TRPM2-ΔC (34). TRPM2-ΔC as well as point mutants at hydrophobic residues in the coiled-coil region have much smaller ADP-ribose-activated whole-cell currents (34). Deletions within and truncations of the coiled-coil domain of TRPM4 almost completely eliminated Ca^{2+}-activated whole-cell currents at +100 mV (37). The truncations resulted in a shift of the activation potential to extremely high positive voltages compared with the wild-type protein. As in our studies of TRPM8, this C-terminally truncated TRPM4 was still localized to the plasma membrane. The available data on TRPM2 and TRPM4 therefore largely agree with our data on TRPM8, although deletion of the TRPM2 coiled-coil affects assembly and trafficking, whereas in our insect cell system, deletion of the TRPM8 coiled-coil does not significantly impair assembly and plasma membrane localization.

In the case of TRPM8, fusion of the coiled-coil region to a transmembrane helix, either S6 of TRPM8 (35) or the transmembrane domain of CD8 (36), produces a dominant-negative effect when coexpressed with wild-type TRPM8. Also, the L1089P mutation within the coiled-coil produces an inactive TRPM8 (35), which does not interfere with menthol-induced whole-cell currents when coexpressed with wild-type TRPM8 in human embryonic kidney cells, suggesting that wild-type TRPM8 prefers to homotetramerize. Another group found that deletion of the TRPM8 coiled-coil prevented TRPM8 expression in HEK293T cells or *Xenopus* oocytes (36). Our data show that TRPM8-ΔC1070 is expressed, forms tetramers, and localizes to the plasma membrane. It is likely our TRPM8 overexpression system in insect cells grown at 27 °C helps drive channel tetramerization even in the absence of the tetramerizing C-terminal coiled-coil. The sufficiency of the transmembrane domain for tetramerization is not surprising in light of its similarity to voltage-gated potassium channels that are also active as tetramers. From the structure of a Shaker family potassium channel (5) we calculated that helices S1–S6 of each monomer interact to form an extensive interface that buries almost 8,000 $Å^2$ of surface area. In fact, overexpressed Shaker channels can tetramerize through their transmembrane domain in the absence of the cytosolic tetramerization T1 domain (38, 39).

The fact that the ΔC1070 construct without the C-terminal coiled-coil still tetramerizes and traffics to the plasma membrane in our insect cell expression system allowed us to determine that the coiled-coil is also necessary for channel activation. Therefore, the TRPM8 coiled-coil has two separate roles in TRPM8 activity. First, it can help direct subunit assembly into functional channels providing specificity and stability beyond the transmembrane region. Second, it is also necessary for channel activation in response to ligands or cool temperatures. Previous results also suggest that the role of the coiled-coil goes beyond just assisting in subunit assembly because its substitution with designed coiled-coils does not produce active channels (36).

Our results with the ΔC992 deletion constructs agree with previous studies indicating that the role of the TRP domain is in channel gating because the deletion of the TRP domain does not prevent assembly and localization. The TRP domain, located between residues 990–1025, contains a combination of basic and hydrophobic residues that are important for channel activation by PIP_2 (26) and agonists like menthol and icilin (24), respectively. Mutations Y1005A and L1009R blocked activation by menthol without altering the temperature sensitivity (24). High concentrations of PIP_2 can directly activate TRPM8, and mutations of conserved basic residues Lys-995, Arg-998, and Arg-1008 decrease TRPM8 sensitivity to PIP_2. The basic residues are conserved in almost all TRPC, -M, and -V family members, and similar losses of sensitivity have been observed for TRPV5 and TRPM5 (26). Although TRPM4 is also sensitized by PIP_2, mutagenesis data indicate that TRPM4 binds PIP_2 using a predicted pleckstrin homology domain in the C terminus, rather than the TRP box (40). At physiologic concentrations, PIP_2 depletion leads to TRPM8 desensitization (25), similar to TRPV1 (27, 41, 42), which also interacts with phosphoinositides through its C terminus (43, 44). Based on our results showing the synergy between PIP_2 and icilin and previous studies on the role of the TRP domain in TRPM8 response to various agonists including PIP_2, icilin, and menthol (24, 26), it is clear that the integrity of the TRP domain is needed for the response to most, if not all, TRPM8 agonists. Direct binding of menthol to residues in transmembrane segments S2 and S4 and the S4-S5 linker has already been observed (21), and biochemical demonstration of direct ligand interaction will be necessary to confirm whether the TRP domain also directly interacts with any of the TRPM8 ligands.

Tetramerization, transport to the plasma membrane, and a functional sensor and gate are activities required for TRPM8 to function as the cold receptor in sensory neurons. Distinct regions of the protein are important for regulating these behaviors. The transmembrane region that forms the channel through the plasma membrane is sufficient for tetramerization. The N-terminal region composed of residues 40–86 is involved in targeting TRPM8 to the plasma membrane. At the other end, the C terminus containing the TRP and coiled-coil domains is required for proper gating of the channel. Channel gating is in turn modulated by the interplay of bound agonists (menthol and icilin), phospholipids (PIP_2), pH, membrane voltage, and temperature. Specific activities have now been assigned to different regions, and this will facilitate future structural and functional studies on TRPM channels.

Acknowledgments—We thank William J. Tyler and Polina Lishko for assistance and advice with the electrophysiology; Dave Smith of the Harvard University Department of Molecular and Cellular Biology Imaging Center for assistance with the confocal microscopy and immunofluorescence; and Erik Procko, Wilhelm Weihofen, and other members of the Gaudet laboratory for critical input.

REFERENCES

1. Montell, C. (2005) *Sci. STKE* **2005,** 1–24
2. Nilius, B., and Voets, T. (2005) *Pflugers Arch. Eur. J. Physiol.* **451,** 1–10
3. Clapham, D. E. (2003) *Nature* **426,** 517–524
4. Jiang, Y., Lee, A., Chen, J., Ruta, V., Cadene, M., Chait, B. T., and Mackinnon, R. (2003) *Nature* **423,** 33–41
5. Long, S. B., Campbell, E. B., and Mackinnon, R. (2005) *Science* **309,** 897–903
6. Montell, C. (2001) *Sci. STKE* **2001,** 1–17

7. Fleig, A., and Penner, R. (2004) *Trends Pharmacol. Sci.* **25,** 633–639
8. Harteneck, C. (2005) *Naunyn-Schmiedeberg's Arch. Pharmacol.* **371,** 307–314
9. Kraft, R., and Harteneck, C. (2005) *Pflugers Arch. Eur. J. Physiol.* **451,** 204–211
10. McKemy, D. D., Neuhausser, W. M., and Julius, D. (2002) *Nature* **416,** 52–58
11. Peier, A. M., Moqrich, A., Hergarden, A. C., Reeve, A. J., Andersson, D. A., Story, G. M., Earley, T. J., Dragoni, I., McIntyre, P., Bevan, S., and Patapoutian, A. (2002) *Cell* **108,** 705–715
12. Colburn, R. W., Lubin, M. L., Stone, D. J., Jr., Wang, Y., Lawrence, D., D'Andrea, M. R., Brandt, M. R., Liu, Y., Flores, C. M., and Qin, N. (2007) *Neuron* **54,** 379–386
13. Dhaka, A., Murray, A. N., Mathur, J., Earley, T. J., Petrus, M. J., and Patapoutian, A. (2007) *Neuron* **54,** 371–378
14. Bautista, D. M., Siemens, J., Glazer, J. M., Tsuruda, P. R., Basbaum, A. I., Stucky, C. L., Jordt, S. E., and Julius, D. (2007) *Nature* **448,** 204–208
15. Reid, G. (2005) *Pflugers Arch. Eur. J. Physiol.* **451,** 250–263
16. Caterina, M. J., Schumacher, M. A., Tominaga, M., Rosen, T. A., Levine, J. D., and Julius, D. (1997) *Nature* **389,** 816–824
17. Brauchi, S., Orta, G., Salazar, M., Rosenmann, E., and Latorre, R. (2006) *J. Neurosci.* **26,** 4835–4840
18. Voets, T., Droogmans, G., Wissenbach, U., Janssens, A., Flockerzi, V., and Nilius, B. (2004) *Nature* **430,** 748–754
19. Brauchi, S., Orio, P., and Latorre, R. (2004) *Proc. Natl. Acad. Sci. U. S. A.* **101,** 15494–15499
20. Hui, K., Guo, Y., and Feng, Z. P. (2005) *Biochem. Biophys. Res. Commun.* **333,** 374–382
21. Voets, T., Owsianik, G., Janssens, A., Talavera, K., and Nilius, B. (2007) *Nat. Chem. Biol.* **3,** 174–182
22. Chuang, H. H., Neuhausser, W. M., and Julius, D. (2004) *Neuron* **43,** 859–869
23. Andersson, D. A., Chase, H. W., and Bevan, S. (2004) *J. Neurosci.* **24,** 5364–5369
24. Bandell, M., Dubin, A. E., Petrus, M. J., Orth, A., Mathur, J., Hwang, S. W., and Patapoutian, A. (2006) *Nat. Neurosci.* **9,** 493–500
25. Liu, B., and Qin, F. (2005) *J. Neurosci.* **25,** 1674–1681
26. Rohacs, T., Lopes, C. M., Michailidis, I., and Logothetis, D. E. (2005) *Nat. Neurosci.* **8,** 626–634
27. Lishko, P. V., Procko, E., Jin, X., Phelps, C. B., and Gaudet, R. (2007) *Neuron* **54,** 905–918
28. Phelps, C. B., Procko, E., Lishko, P. V., Wang, R. R., and Gaudet, R. (2007) *Channels* **1,** 148–151
29. Dragoni, I., Guida, E., and McIntyre, P. (2006) *J. Biol. Chem.* **281,** 37353–37360
30. Perraud, A. L., Schmitz, C., and Scharenberg, A. M. (2003) *Cell Calcium* **33,** 519–531
31. Launay, P., Cheng, H., Srivatsan, S., Penner, R., Fleig, A., and Kinet, J. P. (2004) *Science* **306,** 1374–1377
32. Lis, A., Wissenbach, U., and Philipp, S. E. (2005) *Naunyn-Schmiedeberg's Arch. Pharmacol.* **371,** 315–324
33. Zhang, L., and Barritt, G. J. (2004) *Cancer Res.* **64,** 8365–8373
34. Mei, Z. Z., Xia, R., Beech, D. J., and Jiang, L. H. (2006) *J. Biol. Chem.* **281,** 38748–38756
35. Erler, I., Al-Ansary, D. M., Wissenbach, U., Wagner, T. F., Flockerzi, V., and Niemeyer, B. A. (2006) *J. Biol. Chem.* **281,** 38396–38404
36. Tsuruda, P. R., Julius, D., and Minor, D. L., Jr. (2006) *Neuron* **51,** 201–212
37. Nilius, B., Prenen, J., Tang, J., Wang, C., Owsianik, G., Janssens, A., Voets, T., and Zhu, M. X. (2005) *J. Biol. Chem.* **280,** 6423–6433
38. Minor, D. L., Lin, Y. F., Mobley, B. C., Avelar, A., Jan, Y. N., Jan, L. Y., and Berger, J. M. (2000) *Cell* **102,** 657–670
39. Zerangue, N., Jan, Y. N., and Jan, L. Y. (2000) *Proc. Natl. Acad. Sci. U. S. A.* **97,** 3591–3595
40. Nilius, B., Mahieu, F., Prenen, J., Janssens, A., Owsianik, G., Vennekens, R., and Voets, T. (2006) *EMBO J.* **25,** 467–478
41. Liu, B., Zhang, C., and Qin, F. (2005) *J. Neurosci.* **25,** 4835–4843
42. Stein, A. T., Ufret-Vincenty, C. A., Hua, L., Santana, L. F., and Gordon, S. E. (2006) *J. Gen. Physiol.* **128,** 509–522
43. Brauchi, S., Orta, G., Mascayano, C., Salazar, M., Raddatz, N., Urbina, H., Rosenmann, E., Gonzalez-Nilo, F., and Latorre, R. (2007) *Proc. Natl. Acad. Sci. U. S. A.* **104,** 10246–10251
44. Kwon, Y., Hofmann, T., and Montell, C. (2007) *Mol. Cell* **25,** 491–503

The Role of the N Terminus and Transmembrane Domain of TRPM8 in Channel Localization and Tetramerization

Christopher B. Phelps and Rachelle Gaudet

J. Biol. Chem. 2007, 282:36474-36480.
doi: 10.1074/jbc.M707205200 originally published online October 1, 2007
